~~An intercomparison~~ A comparison of Large-Eddy Simulations of the Martian daytime convective boundary layer: sensitivity study and challenges

Tanguy Bertrand[1], Aymeric Spiga[1], Scot Rafkin[2], Arnaud Colaitis[1], François Forget[1], and Ehouarn Millour[1]

[1]Laboratoire de Météorologie Dynamique (UPMC/CNRS), Paris, France
[2]Southwest Research Institute, Boulder, CO, USA

Correspondence to: Tanguy Bertrand (tanguy.bertrand -a- lmd.jussieu.fr)

Abstract. Large-Eddy Simulations (LES) for Mars resolve the Planetary Boundary Layer (PBL) turbulent dynamics by using a very fine horizontal resolution of a few tens of meters. LES modeling is becoming a more and more useful tool to prepare the robotic exploration of Mars by providing means to evaluate the intensity of convective plumes and vortices, horizontal wind gustiness, and turbulent fluctuations of temperature in the Martian PBL. In such context, and given the relative paucity of turbulence-related measurements on Mars, ~~an intercomparison~~ a comparison of LES models is a fruitful way to evaluate the models' predictions and to indicate possible areas of improvement. Thus, ~~to prepare the~~ in the context of the landing of the ExoMars Schiaparelli lander (also named ExoMars Demonstrator Module, EDM) ~~, scheduled for~~ in October 2016, the results of the Laboratoire de Météorologie Dynamique (LMD) and ~~South-West~~ Southwest Research Institute (SwRI) LES models have been compared. The objective of this study is to determine the range of uncertainties, and dispersions, of the two numerical models' predictions, for the critical phase of the spacecraft's descent in the Martian daytime turbulent PBL. First, a strategy is defined to ensure similar radiative forcing in both the LMD and SwRI models. Then, LES are performed over a flat terrain with and without large-scale ambient horizontal wind. The LMD and SwRI Martian LES models predict similar temporal evolution of the PBL and organization in the horizontal and vertical wind fields. However, the convective motions in the daytime PBL are more vigorous by a factor 1.5-2 in SwRI results than in LMD results, independently of the presence or not of ambient horizontal wind. ~~This discrepancy is further investigated~~ We explore further these discrepancies through sensitivity studies to surface conditions, ambient wind, and airborne dust loading. Finally, we discuss about their possible origins and about the challenges of LES intercomparison in general.

1 Introduction

In the Martian atmosphere, the Planetary Boundary Layer (PBL) depth can reach about ten kilometres above the surface in the daytime, when it is prone to intense turbulent convection associated with strong radiative warming of the surface (e.g., **????**). Conversely, in the night, convective motions are inhibited by surface radiative cooling, which creates a near-surface stable layer, subsequently removed within about an hour after sunrise. As a result, the depth of the daytime PBL on Mars

undergoes strong variations with both incoming sunlight (as determined by local time, season, and dust opacity) and surface thermophysical properties (thermal inertia and albedo). Furthermore, the regional variability of the PBL depth on Mars is controlled by ~~altimetry~~ altitude (**??**), as well as ambient (i.e. regional and large-scale) wind (**?**).

The turbulent PBL is a very dynamic part of the Martian atmosphere, characterized by abrupt changes in temperature, pressure, wind, and aerosols. These PBL variations have been characterized mostly by instrumented landers and rovers such as the Viking spacecraft in the late 1970s (**?**), Pathfinder in the late 1990s (**?**), Mars Exploration Rovers and Mars Phoenix in the 2000s (**??**) – while Martian orbiters provided measurements of PBL depth (**?**), as well as imagery of PBL-induced phenomena such as dust devils (**?**) and cloud streets (**?**). Despite this set of observations, the coverage of the Martian PBL activity has remained sparse thus far compared to e.g. what has been made available for the Earth's PBL.

A complementary approach to observations to study Mars' PBL is the use of numerical modeling. Three-dimensional turbulence-resolving Large-Eddy Simulations (LES) have been employed since the early 2000s to assess the intense daytime PBL dynamics on Mars (**????**), which includes convective vortices generating the observed dust devils (**?**, for a review). In LES, using a horizontal resolution of some tens of meters permits ~~to resolve the~~ the resolution of the larger turbulent eddies, which are the source of most of the energy transport within the PBL (**?**). Given the relative paucity of PBL measurements on Mars, LES models are of crucial importance to help understanding the PBL processes, thus broadening our knowledge of the atmospheric circulations on Mars at all scales (from planetary scales to turbulent scales).

LES have also become powerful tools to prepare Martian exploration, since they are being used to characterize atmospheric hazards in the Entry, Descent and Landing (EDL) phase of a spacecraft, and in turn to help define the design of the landing system (**???**). This is especially true for small spacecrafts landing with a parachute system, which may be more easily subject to oscillations than massive spacecrafts such as MSL or Mars 2020. In addition, LES results may be crucial for future Martian missions, e.g. for the navigation system of autonomous robotic flying exploration vehicles, such as Mars Helicopter. Finally, any future instrument designed to study the PBL will need LES results in order to predict the atmospheric turbulence it will encounter and assess its performance.

At the time of writing, several LES models for Mars are available in the community to characterize Martian PBL dynamics (cf. reference above, plus **????**). All published LES describe the same qualitative behaviour: a deeply convective PBL during daytime, starting with a gradual growth of the mixed layer in the morning and ending with a rapid stabilization in the end of the afternoon, associated with polygonal horizontal cells, thermal plumes and convective vortices. However, not only do the various models ~~do~~ not share the same characteristics, but quantitative estimates were found to differ when predictions from various Martian LES models were compared for EDL studies (**?**).

A systematic intercomparison between ~~at least two~~ all existing Martian LES models is still yet to be carried out to further characterize those differences. ~~This is what is proposed in~~ Such an effort to compare all available models is beyond the scope (in term of human, time and funding resources) of the present study ~~.~~ (see section **??**). Here we propose, as a necessary first step towards a true intercomparison, an unprecedented systematic comparison between two existing Martian LES models based on two distinct hydrodynamical solvers.

The need to evaluate the differences predicted by two distinct Martian LES is threefold:

1. Contrary to observational data, an estimate of the uncertainties of LES ~~predictions~~ diagnostics is still lacking. This is especially critical for the studies of atmospheric hazards during EDL, given the central role that LES ~~predictions~~ diagnostics play in those studies and the relative paucity of available data to characterize the Martian PBL dynamics (e.g. for vertical winds). Comparing LES models would ~~thus enable to identify the uncertainties in their diagnostics~~provide guidance on the range of model variance (i.e. the spread in modeling results for a similar Martian site and season), thereby enabling an optimal EDL design for both landing spacecraft and definition of landing ellipse.

2. Carrying out a LES ~~intercomparison~~ comparison would highlight discrepancies between results and help to identify the specific areas in which model improvements would be the most helpful. This overarching goal is beneficial for the whole Martian science. For instance, turbulent wind variability (i.e. "gustiness") plays an important role in controlling dust lifting on Mars (e.g., **?**, and references therein). Since turbulent wind measurements on Mars are very incomplete, LES predictions are still being an important source to assess the wind conditions on Mars associated with dust lifting (**?**). More generally, the continued development of Martian LES models is also of crucial importance to better understand the mechanisms responsible for heat and momentum transfer both by daytime PBL mixing and surface-atmosphere interactions. Following the tendency drawn by terrestrial studies, Martian LES predictions are more and more used to build and improve PBL parameterizations in Global Climate Models (GCMs) for Mars (**?**).

3. Since Martian LES rely on hydrodynamical solvers inherited from terrestrial studies, confronting those models to the intense PBL convection on Mars (compared to the Earth, cf. **?**) provides a stringent test for those solvers. ~~An intercomparison study of~~ A comparison study of two or ideally more Martian LES will ultimately be a strong driver of improvement for the atmospheric models used to carry out LES on Earth, and in an increasingly diverse range of planetary conditions (e.g. Venus LES, **???**).

In this paper, we compare the LES results obtained by, on the one hand, the Laboratoire de Météorologie Dynamique (LMD) Martian mesoscale model (**??**) and, on the other hand, the ~~SouthWest~~ Southwest Research Institute (SwRI) Martian mesoscale model (**??**). We develop a strategy which makes our ~~intercomparison~~ comparison study the first one of its kind for Mars: we ensure that similar physical constants and radiative forcing are employed in both models before performing a comparative analysis of LES results and conclude on the performance of the two dynamical solvers in predicting Mars' PBL convective motions. We further complement this ~~intercomparison~~ comparison study by an exploration of the sensitivity of the convective PBL predicted by the LMD LES to surface thermophysical properties (e.g. albedo), ambient wind, and atmospheric dust loading.

~~We perform the present LES intercomparison~~ The present LES comparison has been performed in the context of the European Space Agency (ESA) ExoMars 2016 mission (hereinafter referred as ExoMars) with the aim of providing constraints for the EDL of the ExoMars Demonstrator Module (EDM, also named Schiaparelli). LES modeling ~~is therefore~~ has therefore been performed at the ExoMars landing site, namely in the Terra Meridiani region (latitude $-1.82°$N, longitude $-6.15°$E), ~~for the landing scheduled~~ at the landing date in northern autumn (solar longitude $L_s = 244°$).

In ~~Section~~ section **??**, we describe the LMD and SwRI models used in this LES ~~intercomparison~~comparison. In section **??**, we provide details on the ~~intercomparison~~ comparison strategy, and how we reached similar radiative forcing both in SwRI and LMD LES. The results of both the Martian LES ~~intercomparison~~ comparison and sensitivity study are discussed in section **??** and **??** respectively. Finally, in section **??**, we discuss the challenges of LES intercomparison and we suggest a possible path forward for future LES studies. ~~We conclude about the similarities vs. discrepancies between the two models in section ??.~~

2 Models description

We provide here the key points to describe the two models used for our LES ~~intercomparison~~comparison. Further details about each model can be found in the references provided in this section.

Both LMD and SwRI Martian LES models have been built independently by adapting terrestrial mesoscale models to the Martian case, with the coupling of specific physical models (namely, radiative transfer and soil model) initially developed for Martian GCMs:

- LMD LES are performed using the LMD Martian Mesoscale Model (**??**), based on the Weather Research and Forecast (WRF) model and its fully compressible non-hydrostatic dynamical core (**??**), combined with the comprehensive set of physical parametrizations of the LMD GCM (**?**).
- SwRI LES are performed using the Mars Regional Atmospheric Modeling System (MRAMS), a nonhydrostatic Martian mesoscale model developed at SwRI (**??**) and based on the terrestrial RAMS dynamical core (**?**), in which physical parameterizations are inherited from the Martian NASA Ames GCM (**?**).

The two LES models not only use very distinct different radiative transfer and soil ~~model~~ models (inherited from GCM), but also use different dust scattering properties (at the time the runs for this study were carried out, **?** for SwRI LES vs. **?** for LMD LES), which can lead to significant departures in the predictions of atmospheric temperatures.

Although the largest turbulent eddies (contrary to global and regional climate models) are resolved, LES still lack the mixing produced by the unresolved small-scale eddies, which requires the inclusion of parameterizations for subgrid-scale diffusion. In the two models used for this ~~intercomparison~~comparison, the resolved large-eddy ~~Turbulent Kinetic Energy~~ turbulent kinetic energy (TKE) can be used to assess the strength of small-scale mixing in the parameterization, which is usually effective on the three spatial coordinates rather than the sole vertical dimension. The SwRI Martian LES model contains a specific Deardorff diffusion scheme (**?**), also used in the terrestrial version of MRAMS. The LMD LES model uses the strategy adopted for WRF terrestrial LES (**?**), which is similar qualitatively to the one adopted by SwRI with MRAMS – although subgrid-scale mixing coefficients differ between LMD and SwRI LES (see ~~Section~~ section **??** and **??**). Both models use a (qualitatively similar) Richardson-based surface layer to compute surface-atmosphere transfers of heat, momentum, and tracers (transfer coefficients vary with atmospheric stability, see e.g. **?**).

Although the dynamical and physical parts of the LMD and SwRI LES models are different, the simulation framework in both models is similar. To resolve the 3-D convective plumes, cells and vortices, LES are performed on a domain using

periodic boundary conditions, with horizontal and vertical resolutions of a few tens of meters. The radiative transfer models in LES are combined with a horizontally uniform and static dust profile. Surface properties (topography, albedo, thermal inertia) are uniform too in the LES domain. The models typically compute 10 Martian hours during daytime to capture the convective PBL rise, growth and collapse. In both the LMD and SwRI models, a random (noise) perturbation of 0.1 K amplitude is added to the initial temperature field to break its symmetry and help trigger convective motions (**?**).

3 ~~Intercomparison~~ LES comparison methodology

Since the LMD and SwRI models use a combination of very distinct radiative transfer modeling, dust properties, and subsurface modeling, a preliminary preparation of models is necessary to prevent the LES ~~intercomparison~~ comparison from being simply ~~an intercomparison~~ a comparison of radiative transfer schemes, in the radiatively-controlled (by dust and CO_2) Martian environment. This is actually one of the reasons why a systematic intercomparison study between mesoscale models or LES for Mars has not been carried out yet: thus far the models used for comparisons did not use similar radiative forcing, making the analysis of dynamical differences rather cumbersome, although the dispersion of simulated results remained informative about differences between models (e.g. **?**). Conversely, what is aimed at in the present ~~intercomparison study is to assess~~ comparison study is an assessment of the departures in PBL dynamics possibly arising from the use of two distinct LES models – rather than departures resulting from combined differences in the dynamical core and physical parameterizations. To that end, not only we use the closest possible LES settings between LMD and SwRI modeling framework (section **??**), but we also ensure that the same radiative forcing of the atmospheric flow is imposed in the LMD and SwRI models (section **??**), thereby enabling us to conduct consistent dynamical comparisons of both LES models in section **??**. The challenges and subtleties which have arisen when developing this strategy are discussed in section **??**.

3.1 General settings

The main settings used in LMD and SwRI LES are summarized in Tables **??** (model parameters) and **??** (planetary constants). The rationale for those choices is to reach a high level of similarity in both models as far as model domain, planetary constants and initial conditions are concerned.

The computational domain has to be wide enough to contain several convective cells (**?**), in order to derive consistent PBL statistics from LES results. At the same time, the horizontal resolution must be fine enough to enable a good representation of the "large eddy" part of the turbulence spectra. ~~Hence the choice for an horizontal~~ In fact, these two requirements are challenging to achieve for LES simulations (see section **??**). Indeed, a rule of thumb is to design the grid so that the length of the domain side is three times the size of the largest eddy that will be resolved by the simulation. Thus, assuming a maximal PBL height of 10 km on Mars, 30 km would be an appropriate horizontal size for the LES domain. Thus, if we use a horizontal resolution of 50 m~~and~~ , we need 600x600 grid points – which would have raised significantly the computational burden of our study and would have prevented us to carry out the multiple LES runs requested by our study. Here, as a tradeoff, we choose a horizontal resolution of 50 m and 145×145 grid points~~(this configuration provides similar PBL statistics as other configurations with more~~

Parameter	Model settings for the ~~intercomparison~~ comparison
Horizontal grid (x,y)	145×145
Horizontal resolution	50 m
Vertical grid	201 levels (LMD) - 150 levels (SwRI)
Vertical resolution	60 m (LMD) - 80 m (SwRI)
Model top	12 km
Dynamical time step	0.5 s
Region	$-1.82°$N ; $-6.16°$E (Meridiani Planum - ExoMars 2016 landing site)
Solar Longitude	$244°$ (Landing date, northern autumn)
Surface conditions	Albedo: 0.21 - Thermal inertia: 238 tiu (adjusted to 300 tiu in the LMD LES, see ~~Section~~ section **??**)
Dust vertical distribution	Conrath type: $P_0 = 610$ Pa and $\nu = 0.007$
Dust opacity	$\tau = 0.2$ (horizontally uniform and constant over time)
Initial temperature profile	Extracted from LMD-GCM run with uniform dust loading of τ=0.2 at geographical coordinates and L_s of the ExoMars reference landing site (Meridiani region)
Ambient wind	Two cases: 0 and 15 m s^{-1}

Table 1. LMD and SwRI LES models settings and configurations for the ~~intercomparison~~comparison.

c_p (J.kg^{-1}.K^{-1})	r (J.kg^{-1}.K^{-1})	g (m.s^{-2})	ϵ	s_{hc} (J.kg^{-1}.K^{-1})	s_{rho} (kg.m^{-3})	D_s (s)
770	192	3.72	0.99	711	1500	88775.244
Φ	e	sma (AU)	L_{yr} (sol)	S_0 (W.m^{-2})	Ω (rad.s^{-1})	R_M (m)
25.1919	0.09341233	1.52366231	669	1367	7.08821e-5	3390000

Table 2. Physical and planetary constants for the Martian atmosphere, as defined in the models: c_p is the specific heat capacity, r is the specific gas constant, g is the gravitational acceleration, ϵ is the ground emissivity, s_{hc} is the subsurface specific heat and s_{rho} is the subsurface density. D_s is the duration of a sol, Φ is the planet obliquity, e is the eccentricity of the planet orbit, sma is its semi major axis, L_{yr} is the number of sols in one Martian year, S_0 is the solar constant at 1 AU, Ω is the planetary rotation rate and R_M is Mars radius.

~~A model top at 12 km above the local surface is used, high enough to ensure that the boundary layer growth will not be influenced by the position of this model top.~~ . This configuration is based on previous LES modeling which has been shown to provide similar PBL statistics as other configurations with more grid points, as detailed in **?**. Sensitivity to domain size is further discussed in section **??**.

The LES models are run with 150 (SwRI) and 201 (LMD) vertical levels, which yields a vertical resolution of approximately 80 m and 60 m respectively in the vertical dimension. Given the type of vertical coordinates employed in each model (WRF uses mass-based coordinates, a slightly different version of sigma coordinates than what is used in RAMS), this difference of vertical resolution is imposed by the typical set of vertical levels which optimizes the performance of physical parameterizations for each model. However, based on the sensitivity study carried out in **?**, this difference in vertical resolution does not affect significantly the PBL predictions through LES. The key requirement is that the vertical resolution is refined to a few meters close to the surface, which is ensured in both models.

For the chosen grid spacing, the dynamical time step is set to be small enough to ensure numerical stability according to CFL criterion, but it has also to be high enough to reduce the usually expensive computational cost of LES – especially given that sensitivity runs are included in this ~~intercomparison~~ comparison study. Thus, a good trade-off for the LES timestep has been found to be 0.5 s. LES are carried out from local times 06:00 to 18:00. The comparison of the results is mainly performed between 11:00 to 17:00 local time since convective motions are usually amongst the strongest around these local times. Furthermore, this range was convenient to assess ExoMars landing atmospheric conditions since the spacecraft is designed to land in the local-time window of 14:00-16:00.

As is mentioned in the introduction, the LES were performed to assess atmospheric hazards for the ExoMars mission. Therefore both surface thermophysical properties and initial temperature profile reflect the conditions at the expected season (end of northern autumn, areocentric longitude $L_s = 244°$) and location (Terra Meridiani, latitude $-1.82°$N, longitude $-6.15°$E) for the ExoMars landing. Thermal inertia is set to 238 J s$^{-\frac{1}{2}}$ m^{-2} K^{-1} (unit hereinafter referred to as tiu for "thermal inertia unit") and albedo to 0.21 – those values are extracted from the Thermal Emission Spectrometer (TES) nighttime data, averaged over a 1000 km^2 location around the ExoMars landing site. LMD and SwRI runs use the same initial temperature profile at $06:00$ local time, extracted at the season and location of ExoMars' landing, from a run with the LMD GCM (**?**) performed with a constant and uniform dust opacity of 0.2, as well as a Conrath-type dust vertical distribution (as is detailed in **??**).

Both LMD and SwRI LES also use these settings for dust opacity and dust vertical distribution. Setting a dust opacity of 0.2 might be an underestimate for the actual value at this season on Mars (**?**), which ranges $0.3 - 0.5$, but assuming a clear atmosphere ensures the most unstable situation, thus the maximum strength for convection in LES runs~~(see)~~. Since this study's focus is on highlighting differences in convective PBL predictions, a more convective situation yields a more stringent test for LES models.

3.2 Reaching a similar radiative forcing in the two compared models

The two LES models we aim to compare share a fair amount of similar settings, as detailed in section **??**. As is discussed in the beginning of this section **??**, this similarity is necessary but not sufficient to ensure a consistent ~~intercomparison~~ comparison

of the LES predictions for the PBL dynamics on Mars. Despite our efforts, the fact that the LMD and SwRI models employ different radiative transfer schemes and dust properties leads to large temperature differences between the models, which overwhelms – or at least competes with – dynamical differences. It would thus be challenging to ascribe the ~~intercomparison~~ differences to either radiative or dynamical differences.

A complete rewrite of either the LMD or SwRI LES to couple the same set of physical parameterizations is not possible in a reasonable amount of time. Hence the solution we found is to modify a small amount of key parameters in the LMD radiative scheme, so that it replicates SwRI radiative transfer predictions and ensures that the radiative forcing of the PBL in the LMD and SwRI LES are similar. Those key parameters are mostly related to dust optical properties (given the strong radiative control of dust on the Martian atmospheric structure, e.g. **?**) and surface thermophysical properties (albedo, thermal inertia), which controls the surface thermal balance in the Martian environment where atmospheric density is so low that the impact of sensible heat flux on this balance is not prominent (e.g. **?**).

We performed the comparisons and corrections using the single-column version (1D) of the respective physical parameterizations used in the LMD and SwRI LES models. All settings of those 1D models are similar to what is described in Tables **??** and **??** for the LES runs, and correspond to ExoMars landing location and season. For the sake of comparison, the same fine vertical resolution has been chosen for simulations with the LMD and SwRI models. The 1D models do not integrate any hydrodynamical equation: an ambient wind of 10 m s^{-1} is only imposed to obtain a realistic value for the sensible heat flux, whose influence on surface temperature is small but not negligible. ~~Convective adjustment, that is usually included in 1D models to model mixing by turbulent plumes resolved by LES, is turned off in the 1D models as is the case in LES integrations.~~ The radiative response of the LMD and SwRI 1D models is assessed by comparing the obtained equilibrium temperature profiles. A match between the two profiles predicted by the 1D models means that the PBL dynamics in both the LMD and SwRI LES are forced by similar (unstable) gradients of vertical temperature imposed by radiative forcing.

The same initial temperature profile is used in the LMD and SwRI 1D models. This initial profile was obtained by running the LMD 1D model during 50 Martian days (repeating the same day corresponding to $L_s = 244^\circ$ conditions). A simulation duration of 50 Martian days is large enough to reach steady-state equilibrium given the short radiative timescales of the Martian atmosphere (this was checked in practice in our 1D simulations). This profile is then used to initialize both the LMD and SwRI models, which are subsequently run for an additional 50 Martian days to ensure that the steady-state equilibrium is reached. In any case, although using the same initial temperature profile is helpful for consistency, results are not very sensitive to the assumed initial profile, owing to (again) the short radiative timescales of the Martian atmosphere.

In **??** and **??**, we show the two temperature profiles and the surface temperatures obtained by the LMD and SwRI 1D models prior to any correction. To first order, the temperature profiles appear similar. Nonetheless, atmospheric temperatures in the LMD model are found to be $5 - 10$ K colder than SwRI temperatures. This bias extends over almost the entire atmospheric column. In addition, LMD daytime surface temperatures are up to 8 K warmer than SwRI results. This further justifies the approach adopted in this section **??**.

Our working assumption is that, given the central role played by dust on controlling the Martian thermal structure, modifying key dust radiative properties would enable us to obtain a match between the temperature profiles predicted by the LMD and

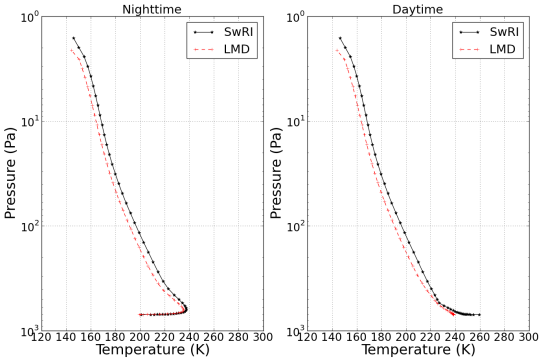

Figure 1. Temperature profiles obtained by LMD (red) before any adjustment and SwRI (black) 1D models at the ExoMars landing site and season. Left are temperatures at local time $00:00$, right are temperatures at $12:00$.

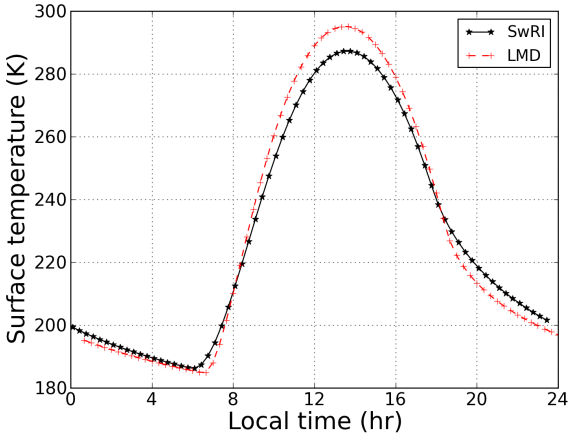

Figure 2. Preliminary comparison of LMD (red) and SwRI (black) surface temperatures at ExoMars landing site, before any adjustment, obtained with 1D models. The 8 K temperature gap around noon highlights the differences between both radiative models.

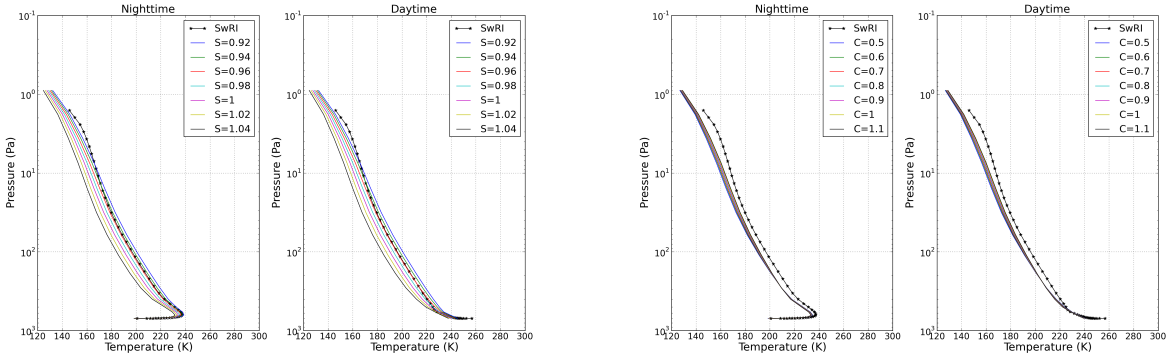

Figure 3. ~~Top~~Left panel: sensitivity of LMD 1D temperature profiles to the dust brightness S. Left are temperatures at local time 00:00, right are at 12:00. SwRI 1D temperature profile is shown for reference in black. ~~Bottom~~Right panel: Same figures, but for sensitivity to the dust thermal infrared opacity C.

SwRI models. We chose to vary 1. the dust extinction efficiency Q_{ext} (or "thermal infrared opacity", at the reference infrared wavelength) and 2. the visible single scattering albedo w_0, which quantifies dust "brightness" (further details and explanations in **??**). For the sake of simplicity, we define the ratios S and C of the corrected value over the reference value for respectively w_0 and Q_{ext} in the LMD model. The higher S, the brighter dust; the higher C, the stronger absorption by dust in the infrared.

?? shows the sensitivity of the temperature profiles to S and C. Here, the comparison of profiles is focused above the PBL because in 1D, the PBL is parameterized while it is resolved in LES (see next section for comparisons within the PBL). We performed a comparative study for all local times, given that LES runs span stability conditions from highly unstable around noon to highly stable in early morning and late afternoon. For the sake of illustration, we show in the aforementioned figures typical nighttime and daytime temperature profiles at local times $0:00$ and $12:00$. In the clear atmosphere case we adopted (setting dust opacity to 0.2), dust brightness S has a strong impact on the temperature profiles: a decrease of 20 K is obtained in nearly the whole atmospheric column when increasing S from 0.92 to 1.04. Indeed bright dust means higher dust albedo, hence increased reflection of solar flux to space, and colder atmosphere and surface. The dust extinction ratio C has a lesser impact (though not negligible) than S on the thermal structure, as shown by **??**. This is expected for a clear atmosphere, where dust absorption in the infrared is not significant enough to cause a strong heating of the atmosphere (contrary to dust storm conditions). This sensitivity study shows that the values of the dust visible scattering albedo and extinction efficiency should be decreased to simulate the effect of dust aerosols both darker and more strongly absorbing in the infrared. The effect of this correction is to warm the atmosphere (both during daytime and nighttime).

As the tuning of these dust parameters does not change significantly the surface temperatures (because of the relatively clear atmosphere considered), the surface thermal inertia has also been changed in the LMD model so that it replicates the SwRI diurnal cycle, at least during daytime when the surface temperatures impact the PBL. Many optimization loops have been performed to replicate in an optimal way the ~~MRAMS-Ames~~ SwRI temperatures at all local times, taking into account

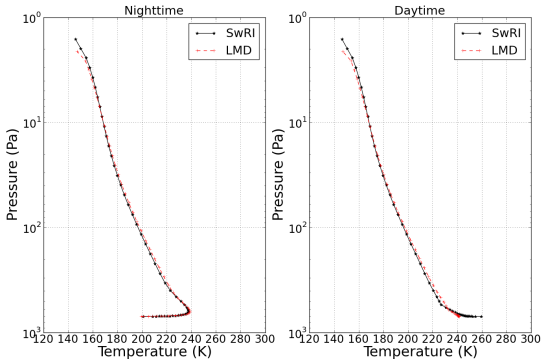

Figure 4. Same as **??** with $S = 94\%$ and $C = 70\%$ in the LMD 1D model.

the change of surface temperature as well. ~~By~~ Values of $S = 94\%$ and $C = 70\%$ are used, in order to bridge the $5 - 10$ K gap between the LMD and SwRI temperature profiles (**??**). In addition, by increasing the thermal inertia up to 300 tiu (which remains close to the surface conditions encountered at ExoMars landing site), we decrease the LMD surface temperatures ~~of~~ by about 8 K around noon and replicate the SwRI daytime surface temperatures, as shown in ~~Section~~ section **??** by **??**. ~~Values of $S = 94\%$ and $C = 70\%$ are used, in order to bridge the $5 - 10$ K gap between the LMD and SwRI temperature profiles ( ) .~~ However, there is still a 20 K gap in the daytime near-surface temperatures that cannot be reduced (over a range of plausible parameters) by optimizing the radiative forcing as it is the case for the rest of the PBL. This suggests that differences in the formulation of surface layer schemes in the two models (see (**?**) for MRAMS and (**?**) for LMD LES) might explain such a difference. This remains to be explored, as discussed in section **??**.

4 Comparison of LES results

This section compares the LMD and SwRI LES results, obtained using the settings described by Table **??** and Table **??**, with the modified radiative transfer properties detailed in section **??** which allow a similar radiative forcing between the two models ($S = 94\%$, $C = 70\%$ and thermal inertia = 300 tiu). Two main test cases are considered: LES devoid of any ambient wind, and LES with an ambient wind of 15 m.s^{-1}, thereby providing typical LES results of Martian daytime boundary convection in windless and windy conditions at the ExoMars landing site.

4.1 Forcing of PBL activity

The PBL activity and its evolution are controlled by the surface temperature and the surface incident solar flux. As described in section **??**, the preliminary steps of convergence of both models enabled a similar forcing to be reached, as shown by **??**. During daytime, discrepancies between LMD and SwRI LES surface temperatures are less than 1 K, and we checked that the shortwave and longwave incident solar flux are similar at all local times. In addition, we ~~also~~ checked that the atmosphere above the PBL

is controlled by similar radiative forcing in both models, as is found in the previous section with the 1D models. With these settings, any difference observed in the LES results (PBL depth, maximum updrafts...) ~~will~~ should not be related to differences in "background" radiative thermal structure, but rather to different dynamical approaches in both models. ~~Furthermore,~~ Other possible sources of differences are discussed in section **??**. For example, as mentioned above, the two models use different PBL ~~near-surface stability~~ surface layer schemes, which ~~may also~~ can impact the results (see ~~and Sections~~sections **??** and ~~??).~~ **??**).

4.2 Comparison of typical LES wind structures

In this section we analyze the turbulent wind structures in order to verify if they are similar in both models and consistent with typical LES diagnostics. Note that the ambient wind is westward in the simulations.

4.2.1 Wind structures and small scale variability

?? shows horizontal sections of vertical winds at about 250 m and 2 km above the surface and at local time 11:00, obtained without ambient wind. Both models predict a horizontal organization of vertical winds into polygonal cells with narrow updrafts on the ridges of the cells and large subsidence in the middle of the cells, with same spatial dimensions and structure sizes. These are a typical pattern of the PBL which remain in conformity with typical LES studies. At 250 m altitude, maximum updrafts and downdrafts reach up to 8 m.s^{-1} and -6 m.s^{-1} in both models, with slightly higher values over few grid points in SwRI results. At 2 km altitude, where updrafts are more vigorous, the differences between both results are more pronounced. LMD LES ~~predict maximum updrafts values~~ predicts a maximum updraft value of 8 m.s^{-1} while SwRI LES results show values twice higher, around 15 m.s^{-1} (see ~~Section~~ section **??**). Because of mass conservation, downdrafts are also found to be more vigorous in the SwRI LES than in the LMD LES.

?? and **??** show horizontal sections of horizontal wind amplitudes at local time 11:00, at about 5 and 250 m above the surface, in the case of an ambient wind of 0 and 15 m.s^{-1} respectively.

In the case without ambient wind, horizontal wind structures are similar in both models and typically show gusts in all directions related to the convective cells in the PBL. However, it can be noticed that the variability at very small scale (i.e. a few grid points apart) is much higher in SwRI results than in LMD results. This higher small-scale variability appears in all SwRI simulations~~and~~. They may be related to the quantitative discrepancies ~~discussed in Section ??~~seen in PBL diagnostics (section **??**) and summarized in Tables **??**-**??**. This is further discussed in section **??**. Here, maximum horizontal wind amplitudes at 5 m above surface are found to be in the range 6-8 m.s^{-1} in both LMD and SwRI LES, although SwRI results also show maximum values at 12 m.s^{-1} over a few grid points. At 250 m above surface, horizontal winds reach 6 m.s^{-1} in both models (9 m.s^{-1} over a few grid points in the SwRI model).

When a sufficiently strong ambient wind is added (typically more than 10 m.s^{-1}), it distorts the organization in polygonal cells and forces the gusts to propagate in the same direction, as shown by **??**. In this case, LMD wind amplitudes are found to be larger than SwRI values, especially 250 m above the surface, although the wind structures remain similar in both LES. Maximum values for horizontal wind are 16-18 m.s^{-1} in both LES.

This difference in altitude is highlighted by **??**, showing the mean profile of horizontal winds in both models between 11:00 and 12:~~00.~~ 00, in the simulation with 15 m.s^{-1} ambient wind. SwRI results show weaker horizontal winds than LMD results in the whole PBL. Although these differences could be related to the different intensity of the convection, they may also be related to the different scheme of near-surface stability. The large differences encountered in the first hundreds of meters reinforce this possibility ~~.~~ (see section **??**). It can also be noted that SwRI results show a deeper mixed layer, which is consistent with the overall weaker winds (momentum is mixed through a deeper layer).

4.3 Comparisons of PBL diagnostics

LES results compared in this section are the PBL depth, the turbulent kinetic energy (TKE) and the maximum updrafts and downdrafts within the PBL, which are key characteristics of the convection inside the Martian PBL. The PBL depth is directly and positively correlated to the intensity of its dynamics while the TKE is a measure of turbulence intensity and is directly related to the transport of heat and momentum through the PBL. An increase of TKE denotes a more turbulent PBL. Updrafts and downdrafts also enable ~~to compare the~~ the comparison of the intensity of the PBL turbulence in both models. Table **??** and Table **??** summarize the results.

4.3.1 Planetary boundary layer height

?? shows that the daytime PBL depth grows faster and reaches a higher vertical extent in the SwRI LES than in the LMD LES. By the end of the afternoon, the PBL depth reaches 7.5 km (SwRI) and 4.8 km (LMD) without ambient wind and slightly more in windy conditions. These results confirm that the convection in the SwRI LES is more vigorous. In fact, the maximum PBL depth obtained in the SwRI LES is close to the highest values that could be found on Mars and measured through ~~radio-occultations, which are~~ radio occultation, which is about 8-10 km (**?**). It should be pointed out, however, that these simulations contain none of the realistic physics that would tend to suppress a PBL, notably large-scale subsidence or regional circulations (e.g. as experienced in Gale Crater, see **?**). The turbulent convection is active until the end of the afternoon (typically 16:30-17:00) and suddenly stops (the PBL collapses) when the surface becomes colder than the atmosphere above it (nighttime inversion). For some of the simulations, this occurs before 17:00, explaining the sharp drop in **??**.

4.3.2 Turbulent kinetic energy

The differences in the vertical extent of PBL mixing between both LES can also be inferred from the variations of (resolved) TKE, as shown by **??**. Although the convective activity rapidly declines at same local time 17:00 and the maximum TKE values occur around same local times 13:00-14:00 in both models, larger TKE values are found in the SwRI LES, in consistency with previous results,. Without ambient wind, the maximum TKE in the PBL reaches 12 m^2.s^{-2} around 1.5 km altitude in LMD results, while it reaches about 21 m^2.s^{-2} around 3.5 km altitude in SwRI results, a factor of two more intense. Similar differences are found in the LES with windy ~~condition~~conditions.

LES without ambient wind	LMD	SwRI	Difference (%)
PBL ~~Height~~ height (km)	4.8	7.5	56
Turbulent ~~Heat Flux~~ heat flux (K.m.s^{-1})	< 1.25	< 3.2	156
Turbulent ~~Kinetic Energy~~ kinetic energy (m^2.s^{-2})	< 12	< 21	75
Maximum ~~Updraft Speed~~ updraft speed (m.s^{-1})	< 15	< 24	60
Maximum ~~Downdraft Speed~~ downdraft speed (m.s^{-1})	< 8	< 12	50

Table 3. Maximum PBL diagnostics values from the LMD and SwRI LES without ambient wind

4.3.3 Maximum speed for convective updrafts

In line with previous results, **??** shows that maximum updraft speeds obtained from SwRI LES are higher than those from LMD LES, with a ratio of about 1.5-1.8, all over the mixing layer depth between local times 11:00 and 17:00. In LES without ambient wind, maximum speeds reach 13-15 m.s^{-1} in LMD results around local times 12:00 – 14:00 between altitudes 2 to 4 km while they reach 20-24 m.s^{-1} in SwRI results between altitudes 2 to 6 km at same local times. In windy conditions, maximum updraft speeds in both LMD and SwRI LES remain in similar ranges. This is expected given that SwRI has finer structure (narrower updrafts, presumably less diffusive).

4.3.4 Maximum speed for convective downdrafts

In both LES, maximum updraft speeds (**??**) are in comparison larger by a factor 2 than maximum downdraft speeds (**??**). This is a consequence of the organization of turbulence in cells with narrow updrafts and broader downdrafts. Both LES predict maximum downdraft between local times 13:00 and 15:00. Without ambient wind, downdraft up to 8 m.s^{-1} are predicted by the LMD LES from 200 m to 5 km above the surface while the SwRI LES predicts values up to 12 m.s^{-1}. In the LES with ambient wind, these values slightly increase to 9 m.s^{-1} and 15 m.s^{-1} respectively.

4.3.5 Distributions of vertical wind speeds

?? and **??** show the distribution of vertical wind speeds obtained between local times 13:00-14:00 and altitudes 250-5000 m, for both LES without and with ambient wind respectively. In the windless case, 95% of vertical wind speeds are in the [-6,6] m.s^{-1} range for LMD and [-9,9] m.s^{-1} for SwRI. In the windy case, 95% of vertical wind speeds are in the [-7,7] m.s^{-1} range for LMD, and [-11,11] m.s^{-1} for SwRI. Therefore, the strongest vertical winds represent a very low probability. As an example, in the SwRI LES, both the maximum downdraft value of 11 m.s^{-1} and the maximum updraft value of 28 m.s^{-1} represent less than 0.01% of all values.

LES with 15 m.s^{-1} ambient wind	LMD	SwRI	Difference (%)
PBL ~~Height~~ height (km)	5.3	8.1	53
Turbulent ~~Heat Flux~~ heat flux (K.m.s^{-1})	< 1.7	< 3.4	100
Turbulent ~~Kinetic Energy~~ kinetic energy (m^2.s^{-2})	< 15	< 34	126
Maximum ~~Updraft Speed~~ updraft speed (m.s^{-1})	< 15	< 22	46
Maximum ~~Downdraft Speed~~ downdraft speed (m.s^{-1})	< 9	< 15	60

Table 4. Maximum PBL diagnostics values from the LMD and SwRI LES with 15 m.s^{-1} ambient wind

5 Sensitivity simulations

This section presents a sensitivity study of the Martian daytime PBL properties in the LMD LES model to dust loading, surface albedo, ambient wind and subgrid scale diffusion coefficient, using the same reference settings as described in ~~Section~~ section **??**, without ambient wind. This enables to ~~better understand the mechanisms and the~~ explore the role of forcing ~~in~~ of the Martian PBL ~~, and allows further investigation of the discrepancies observed between SwRI and LMD~~ and to assess if an uncertainty of one parameter can explain the discrepancies evidenced between the LMD and MRAMS LES results. Furthermore, ~~it deserves an entire section, since it~~ such a sensitivity study has seldom been detailed in the existing literature.

5.1 ~~Sensitivity to subgrid scale diffusion~~

~~Can a difference in the small-scale diffusion schemes in both models be related to the difference of values of PBL depth, maximum TKE and vertical wind speeds detailed in Section ??? To attempt to answer this question, the LMD LES model has been run with different subgrid scale diffusion coefficients (or mixing coefficient). Tested with much lower values than the typical one used (0.15 at LMD, decreased by a factor up to 10^6), the PBL diagnostics remain similar with a decrease of PBL height of less than 5% in the afternoon. Same conclusions apply when analyzing the maximum TKE or wind speeds, confirming that the small-scale mixing coefficient has a negligible impact on the development of the convective PBL in the daytime.~~

5.1 Sensitivity to dust opacity

LES have been performed using distinct dust optical depths of 0.2 (reference), 0.6, 1 and 3. Comparing LES predictions in those three cases reveals dramatic differences in the strength of the boundary layer convection. **??** shows how the daytime evolution of boundary layer depth is influenced by dustiness in the Martian atmosphere. Firstly, the mixing layer is of significantly lower vertical extent for higher dust opacities (which is true during the whole day). At local time 14:00, boundary layer depths are respectively 3.8, 3, 2.5, 1.7 km for dust loadings 0.2, 0.6, 1, 3. This behaviour originates from dust absorption of solar radiation in the visible leading to decrease in surface temperature. Moreover, stability in the lowest layers of the atmosphere is enhanced by dust heating, which leads to a less vigorous boundary layer turbulent convection.

Secondly, the PBL is collapsing earlier in the afternoon when dust opacity increases: while the PBL depth is still maximum at local time 17:00 in a clear atmosphere, it starts to slightly decay for a dust opacity at 0.6 and more distinctively decrease for an opacity at 1 (the maximum vertical extent in this case is attained around local time 15:30). The most extreme case (dust opacity at 3) shows a very limited growth of the convective boundary layer, which peaks at the very low value (with respect to Martian standards) of 1.7 km between local times 13:00 and 14:00, before a rapid collapse of the turbulent convection occurs at local time 14:00-14:30.

Both the limitation of convective activity and the displacement of its maximum towards earlier afternoon associated with an increase in dust optical depth can also be assessed by the comparison of maximum (resolved) TKE shown on **??**. Differences in TKE between the clear and extremely dusty cases are about one order-of-magnitude – even differences between the opacity 0.2 and 1 are significant (50 to 60% decrease). It is interesting to note that, in theory, dust radiative heating by absorption in the visible (plus a smaller contribution in the infrared) should cause TKE and updraft speeds to increase with dust opacity. Present LES results with complete radiative transfer show this effect does not significantly compensate the aforementioned influence of dust loading on surface temperature and atmospheric stability. Overall, the dustiness of the Martian atmosphere strongly determines the strength of boundary layer convection and this has important consequences on conditions for EDL systems as ExoMars landing between 14:00 and 16:00. This is exemplified by maximum vertical wind speeds (not shown). Maximum updraft and downdraft values throughout the whole day vary dramatically with dust opacity: updrafts of 15, 12, 10, 4 $m.s^{-1}$ and downdrafts of -9, -7, -5, -2 $m.s^{-1}$ are predicted by LMD LES for dust opacities 0.2, 0.6, 1 and 3. Again, convection for an opacity at 3 is severely limited. Vertical winds are lower at 16:00 than at 14:00 in all cases, but the differences are more prominent between the two local times when more dust is suspended in the Martian atmosphere.

Finally, it is important to note that if the dust opacity values follow a geometric progression which implies a linear increase in atmospheric heating, variations of PBL depth, TKE and maximum winds with dust opacity are not linear. The sensitivity of PBL turbulence to dust opacity is a complex combination of dust influencing surface temperature, atmospheric stability and maximum turbulent heat flux as well as turbulent motions adjusting to those various modified forcings. Only LES employing full radiative transfer can address this complexity.

5.2 Sensitivity to surface albedo

In order to assess the sensitivity of the PBL to surface conditions, the LMD LES has been tested with surface albedo value of 0.1, 0.21 (reference), 0.4 and 0.6. A value of 0.1 is extreme, although not unrealistic, and causes surface temperatures to be significantly warmer, hence boundary layer convection to be more vigorous, as shown by **??** and **??**. A lower albedo not only ~~cause~~ causes the sensible heat flux to be larger, but also the infrared radiative flux emitted by the surface and absorbed by CO_2 and dust in the lowermost atmospheric layers to be larger. The PBL depth predicted by LES is about 20% higher for the 0.1 albedo case, and 35% lower for the 0.4 case, compared to the 0.21 case. Similar conclusions apply for the maximum TKE predicted. The PBL convection on a more reflective surface is very limited, with a height of 1.5 km for an albedo up to 0.6.

5.3 Sensitivity to ambient wind

The sensitivity of the PBL to the ambient wind is addressed by running the LMD LES with 0, 15 (both reference runs) and 25 m.s^{-1} ambient wind. In the afternoon, the wind enhances convection by increasing the surface-atmosphere heat and momentum transfer in the surface layer. Larger wind speeds thus yield higher values for turbulent heat flux, and higher values of TKE (according to the TKE equation). **??** shows that the PBL in windy conditions is especially vigorous between local times 12:00 and 15:30. In addition, the boundary layer convection appears to start earlier in the morning in windy conditions. The maximum TKE predicted by LES in the afternoon is about 20% higher for the 15 m.s^{-1} case (40% for the 25 m.s^{-1} case) compared to the no-wind case. In such conditions, the maximum PBL depth is higher by about 500 m (10%) in the 15 m.s^{-1} case and 700 m (15%) in the 25 m.s^{-1} case, as shown by **??**. Quantitative estimates about maximum vertical winds have to be raised to about 10% and 15% in the 15 m.s^{-1} and 25 m.s^{-1} ambient wind cases respectively, compared to the no-wind estimates (figure not shown).

6 ~~Discussion~~

5.1 Sensitivity to subgrid scale diffusion

Can a difference in the small-scale diffusion schemes in both models be related to the difference of values of PBL depth, maximum TKE and vertical wind speeds detailed in section **??**? In an attempt to answer this question, the LMD LES model has been run with different subgrid scale diffusion coefficients (or mixing coefficients). Tested with much lower values than the typical one used (0.15 at LMD, decreased by a factor up to 10^4), the PBL diagnostics remain similar in the afternoon (**??**). The same conclusions apply when analyzing the maximum TKE or wind speeds, confirming that the small-scale mixing coefficient has a negligible impact on the development of the convective PBL in the daytime. This exploration is incomplete because the discretization of primitive equations in dynamical core may cause the dynamical core to be naturally diffusive (see section **??** for further details), which cannot be controlled by the above-mentioned subgrid-scale mixing coefficients.

5.2 Sensitivity to domain size

The ~~steps of the intercomparison between the~~ LES results can be sensitive to domain size, as was described in section **??**. We ran the model with a much wider domain defined by a 250x250x250 grid, and a model top at 16 km instead of 12 km (horizontal and vertical resolutions remain the same than in the reference case). Results show an increase of the PBL depth of 20-25% (**??**), which is not sufficient to explain the 100% differences observed between both LMD and SwRI LES – although it might explain part of the discrepancy.

6 Challenges of LES intercomparison and suggestions for future studies

This section aims to identify the key challenges of LES intercomparisons and gives suggestions for a possible path forward for future LES studies.

A first difficulty is to determine which models shall be selected to be intercompared. Ideally, the best intercomparison would include all existing models of the community. However, the more models are included, the more multi-dimensional the intercomparison study becomes, with exponential human, time and computing resources needed. Furthermore, the fact that the models have been built independently may lead to several issues: a specific parameter to be explored in the intercomparison may not exist, or may not be easily accessed in all of them; the models have their own strategy for numerical stability, and imposing a unique setting for all the involved models might be detrimental to the quality of their diagnostics; the models use different options, inputs, and outputs (their initialization might actually be a problem on its own within the intercomparison project); the vertical grid of the models may differ, with heights fixed above ground in a sigma-z formulation much different than the sigma-p coordinate used in other models (possibly leading to spurious effects related to one or the other choices for vertical coordinates). A straightforward solution could be to first compare models sharing the same dynamical core, in order to identify any difference related to the physical packages (radiative transfer, mixing, etc...), and then extend the intercomparison to models built on distinct dynamical cores.

One of the difficulties encountered in this paper is the matching of the near-surface temperatures. Surface layer schemes in respectively the LMD and SwRI LES models are based on distinct formulations; we suspect the impossibility to match near-surface temperatures between the two models with our radiative transfer explorations, which suggests that the impact of those differences in surface layer schemes on the near-surface temperature structure in LES is significant and deserves to be explored by a dedicated study. This impact is difficult to evaluate: it affects the magnitude of turbulent activity near the surface, which in turn modifies the sensible heat flux (through the surface layer schemes), which in turn changes the near-surface temperature profile. Future intercomparison studies should acknowledge this issue and try to converge towards similar near-surface temperature profiles.

Another key difference which has been found between the LMD and SwRI ~~LES models~~ models is related to subgrid-scale diffusion. This difference of diffusion is suspected to significantly impact the intensity of the convection within the PBL. Consequently, matching (or, if ever possible, deactivation) of subgrid-scale diffusion schemes between models is an important task to realize consistent intercomparisons. This task is more ambitious than it seems. One difficulty is that subgrid-scale numerical diffusion does not depend on only one parameter. For instance, the LMD LES is based on the WRF dynamical core which is inherently diffusive owing to the chosen discretization of the primitive equations (a diffusive term is added for odd-order advection operators (**?**)). Thus, it is not trivial to completely disable subgrid-scale mixing in a model – in this paper, we tested the LMD LES model sensitivity to the subgrid mixing coefficient, but it has little effect on the results since diffusion terms remain inherent to the formulation of the dynamical core (see **??**). Future LES intercomparisons should further investigate the impact of the subgrid-scale mixing on Martian LES results, which appears of central importance in LES and mesoscale models, and probably even in Global Climate Models. This question has remained eluded in most Martian modeling studies to date.

Another challenge for Martian LES is the size of the modeling domain. As stated by **?**, the horizontal size of the domain must be large enough so that the periodic boundary conditions cannot influence the turbulence computed for the domain interior. Generally speaking, the length of the grid should be three times the size of the largest eddy that will be resolved by the simulation. Since Martian PBL depth typically reach 10 km, the grid size should be around 30 km. In addition, in order to resolve the smaller eddies, the horizontal resolution must be fine enough, typically around tens of meters. Consequently, for a 30 km square LES domain with a 50 m gridspacing, the number of computational locations would then be 600x600. This is challenging to achieve, although largely within reach of modern supercomputers as is demonstrated by a recent study about statistics of dust devils in Martian LES (**?**). In this paper, the model sensitivity to the size of the domain has been tested and results show an increase of PBL depth about 20-25% (see **??**), in line with previous LMD LES studies ((**?**)). Future intercomparisons should be careful about the domain size and top, and test their model with different configurations.

Finally, regarding the strategy we adopted to avoid a comparison of radiative schemes, one suggestion for future Martian LES intercomparisons would be to compare the models with no dust loading at all. This has not been considered in this paper, because the context of the ExoMars mission required LES to be carried out with the most realistic possible temperature profile. LES intercomparisons with a dust-free atmosphere would be a good starting point for future studies – aimed at theoretical discussions and not EDL discussions as in the present paper, since it would enable to compare surface temperatures without the complication of the radiative properties of airborne dust.

7 Discussion

The steps of the comparison between the LMD and SwRI LES models can be summarized as follows: LES have been performed at ExoMars landing site and date using settings as similar as possible. A tuning of the LMD radiative transfer routine has been necessary to ensure a similar radiative response of both LMD and SwRI models to same forcings. This tuning involved slight changes of dust properties (extinction and brightness) and surface thermal inertia (increased from 238 tiu to 300 tiu in the LMD LES), essential to obtain similar daytime surface temperatures in both LES and thus to similarly force the turbulence within the PBL.

The comparison of LES shows similar qualitative results (vertical wind organized into polygonal cells, horizontal gusts) but different quantitative results. SwRI results show values of heat flux, kinetic energy, updraft ~~or~~ and downdraft speeds which are more dispersed, with maximum values higher than LMD results with a ratio between 1.5 and 2, as summarized by Table **??** and Table **??**. This leads to an almost twice more vigorous PBL in the SwRI LES than in the LMD PBL, even though the maximum values only represent a very small fraction of the domain. Results remain similar with or without ambient wind.

It is important to note that all the results and values obtained from both models remain realistic (with the caveat in mind that no measurements of vertical wind in the Martian convective boundary layer are available from previous missions). ~~The LMD LES showed good agreement with other LMD LES performed in the past in~~

The simulations performed with the LMD LES remain typical compared to previous studies performed with the same model. As an example, the PBL height obtained is in the 5-7 km range of what has been obtained in previous studies in conditions

close to the ExoMars landing site ~~, with typical updrafts and downdrafts speed around 8-12 m. s^{-1}, and~~ (e.g similar surface pressure values, see **?**, figure 2 cases b and i). In addition, these values are consistent with radio-occultation measurements (**?**).The boundary layer depths predicted by the SwRI LES model, although clearly in the upper range, are still consistent with those measurements.

The discrepancies observed between both LES ~~can not~~ cannot be explained by differences in boundary conditions or radiative forcing, which are similar in both models (less than 1 K difference). Identifying exactly the origin of those discrepancies is challenging (see section **??**) and beyond the scope of the present study, which is only a first step toward an intercomparison of Martian mesoscale and LES models. In this study, we identified the discrepancies between two Martian LES and drew possible future areas of research to disentangle the causes underlying those discrepancies. It has been found in ~~Section~~ section **??** that SwRI results exhibit a higher variability at a very small scale than LMD results. This could stem from different assumptions in the subgrid-scale diffusion schemes adopted in both LES. On the one hand, the SwRI LES reflects a much weaker subgrid-scale diffusion than the LMD LES, which would put the SwRI LES at greater risk to overestimate maximum vertical winds ("noisy" turbulent signals). On the other hand, the LMD LES appears to have a subgrid-scale diffusion which efficiently removes the accumulation of energy at the grid point scale, although the possibility still exists that this subgrid-scale diffusion might be too strong, yielding underestimated vertical winds. We tested different subgrid scale diffusion coefficients with the LMD LES model but these changes did not significantly affect the PBL. Consequently, it is plausible that the differences observed between both models lie deeper in the assumptions of their small-scale diffusion schemes, in the inherent diffusion within the dynamical cores (e.g., the advection operators and possibly other numerical diffusion assocated with different schemes) or in other dynamic parts of the models (e.g. ~~the distinct discretization~~ distinct discretizations of the hydrodynamical equations). This remains to be explored further in the respective models. Finally, as suggested in ~~Section ??~~ section **??** and **??**, differences in the PBL near-surface scheme used in both models could also impact the LES results.

~~Results in Section~~ Results in section **??** show that the PBL can be strongly affected by large changes of dust loading and surface conditions. In contrast, although the influence of ambient wind on the Martian PBL turbulence is a significant component to be taken into account for EDL studies, results with ambient wind will not change drastically compared to no-wind simulations (here the Martian situation is quite different from the Earth due to the radiative control of the boundary layer). Comparing windy simulations (**??**, **??**) with extreme soil simulations (**??**, **??**) or with dusty simulations (**??**, **??**) shows that windy conditions represent a secondary influence of Martian PBL convection and ~~is~~ are likely to be overcome by changes in the primary forcing of the Martian PBL, that is, radiative control. Turbulent convective activity is enhanced in windy conditions, but this is overwhelmed by the strong suppression of boundary layer growth caused by very dusty conditions.

The conclusions of the ~~intercomparison~~ comparison campaign presented in this paper do not prevent LES from being relevant tools to study the PBL turbulence on Mars and to provide constraints to assess atmospheric hazards encountered by future landing systems, provided caution is exerted along the quantitative lines drawn by the estimates in this paper. Above all, improving the diagnostics provided by Martian LES will require more complete observations of the Martian PBL turbulence in future in situ missions to Mars.

8 Data availability

The SwRI and LMD files, figure data or any other source data of this paper are freely available upon request by contacting T.B. or A.S. (tanguy.bertrand@lmd.jussieu.fr, spiga@lmd.jussieu.fr).

Author contributions. Author contribution

T.B. ~~prepared and~~ and A.C. prepared the comparison of models. T.B. performed the LMD simulations, S.R performed the SwRI simulations. Both T.B. and A.S ~~contributed to the writing of the manuscript.~~ wrote the manuscript, with contributions from S.R., E.M. and F.F.

Competing interests. Competing interests

The authors declare no competing financial interests.

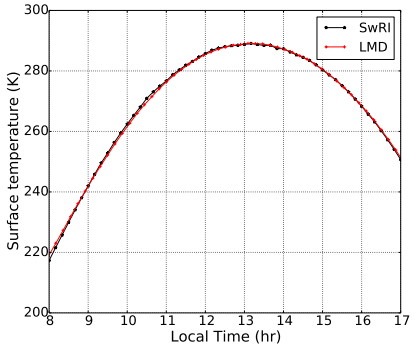

Figure 5. ~~Initial surface conditions~~ Surface temperatures in SwRI (black) and LMD (red) LES models.~~Left are the surface temperatures, middle is the incident short wave solar flux and right is the incident long wave solar flux.~~

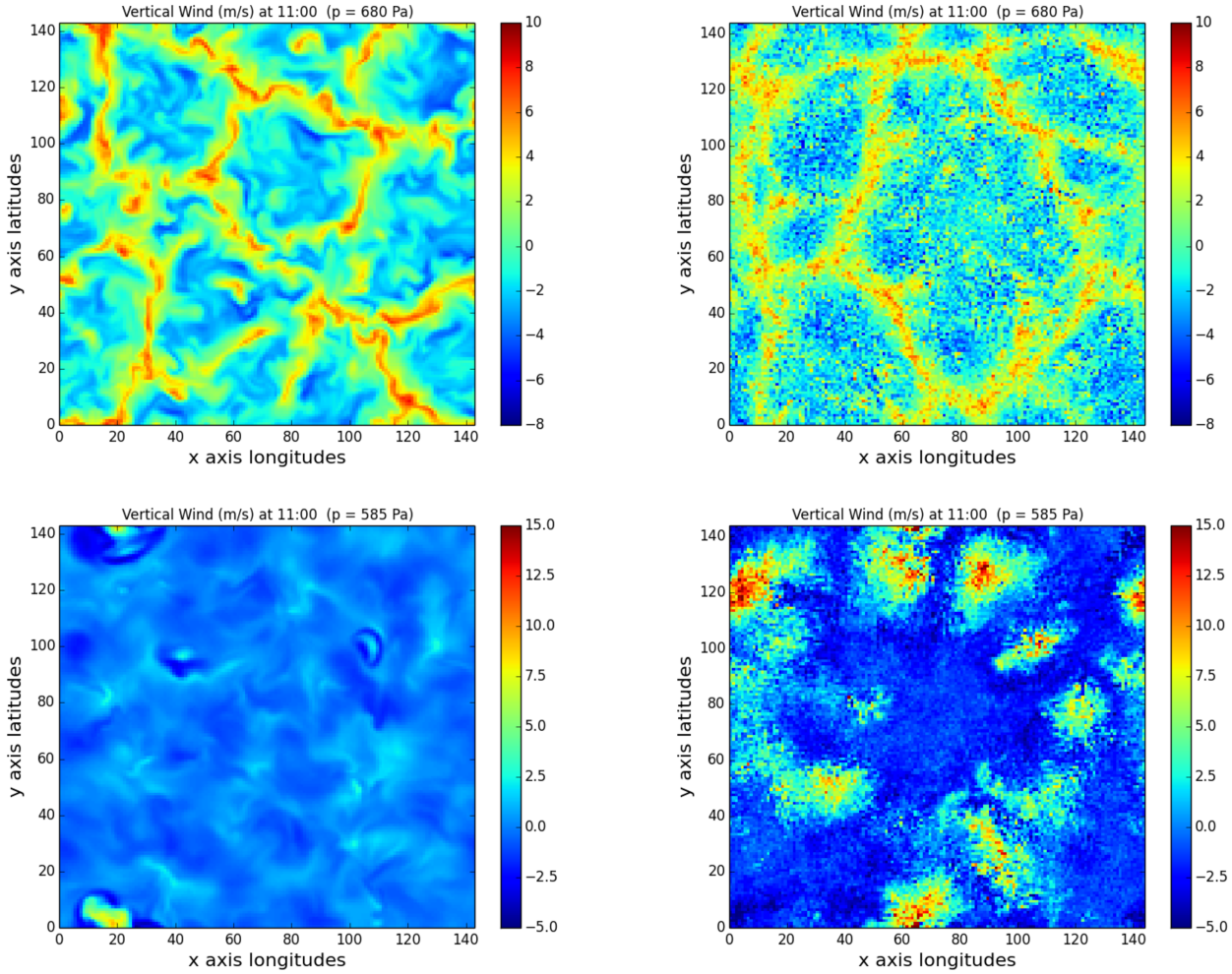

Figure 6. LMD (left) and SwRI (right) horizontal section of vertical velocity at about 250 m (top) and at about 2 km (bottom) above the surface, at local time 11:00. Simulations without ambient wind.

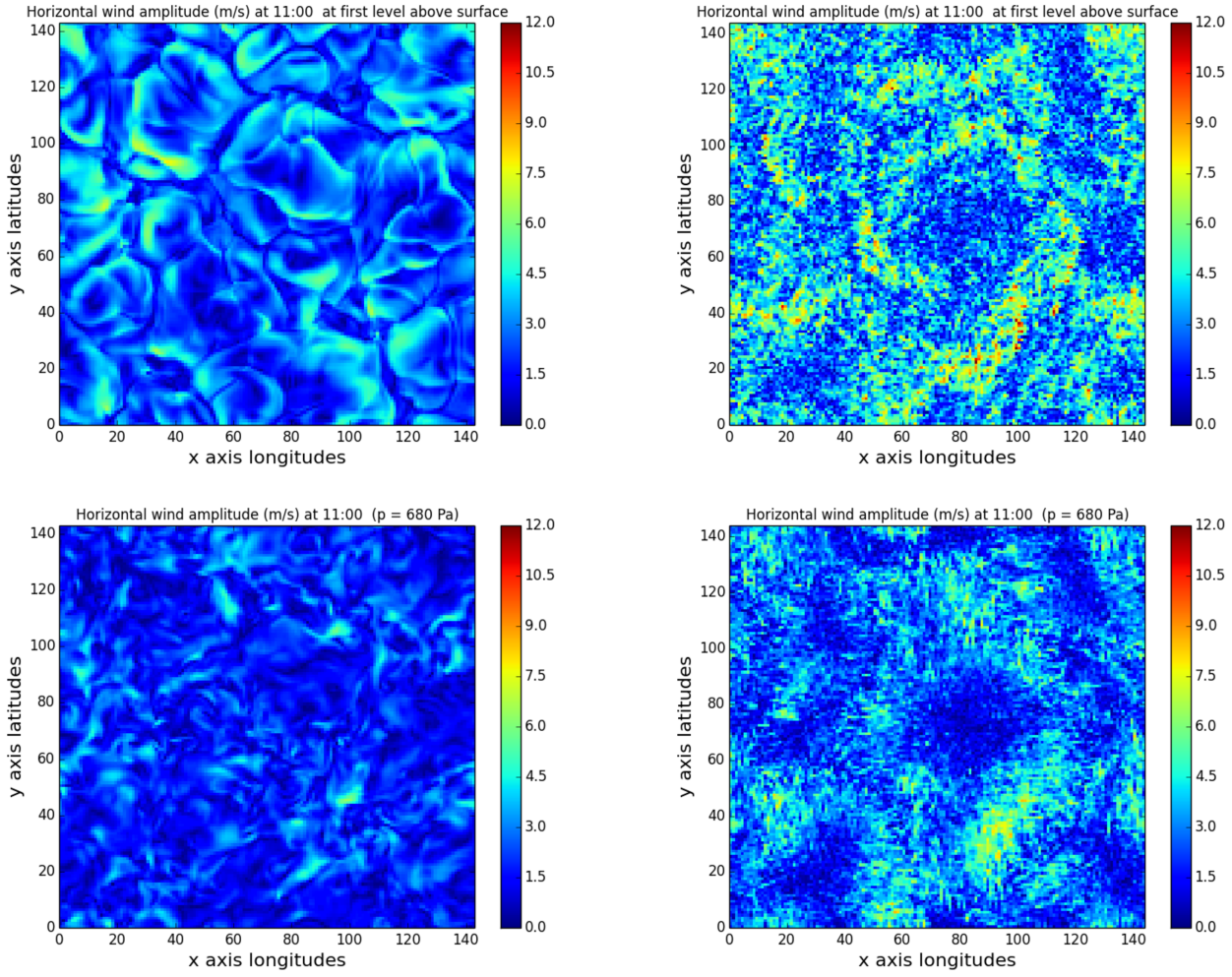

Figure 7. LMD (left) and SwRI (right) horizontal section of horizontal wind amplitudes at first level above surface (top) and at about 250 m above surface (bottom), at local time 11:00. Simulation without ambient wind

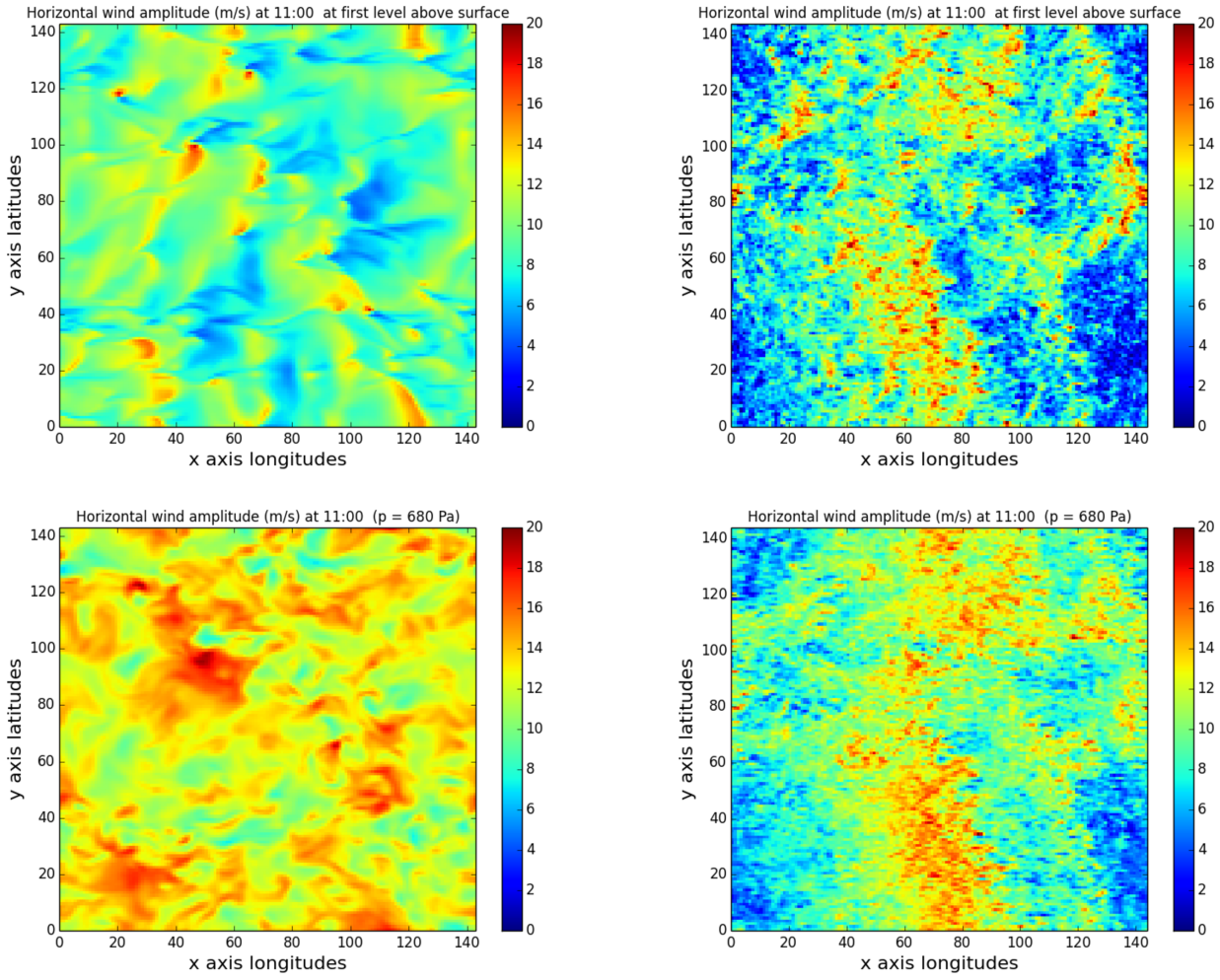

Figure 8. LMD (left) and SwRI (right) horizontal section of horizontal wind amplitudes at first level above surface (top) and at about 250 m above surface (bottom), at local time 11:00. Simulation with 15 m.s^{-1} westward ambient wind.

~~LMD (left) and SwRI (right) horizontal section of vertical velocity at about 250 m (top) and at about 2 km (bottom) above the surface, at local time 11:00. Simulations without ambient wind.~~

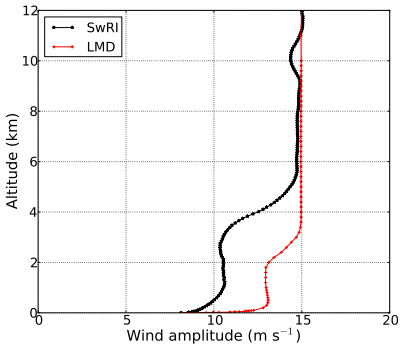

Figure 9. Horizontal wind profile in the SwRI (black) and LMD (red) LES models, between local times 11:00-12:~~00~~00 in the simulation with 15 m.s^{-1} ambient wind.

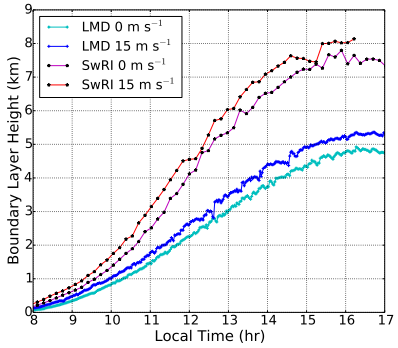

Figure 10. LMD and SwRI variations of boundary layer depth between local times ~~09~~08:00 and 17:00 and altitudes above ground 0 and 9 km. Simulations without ambient wind and with 15 m.s^{-1} ambient wind.

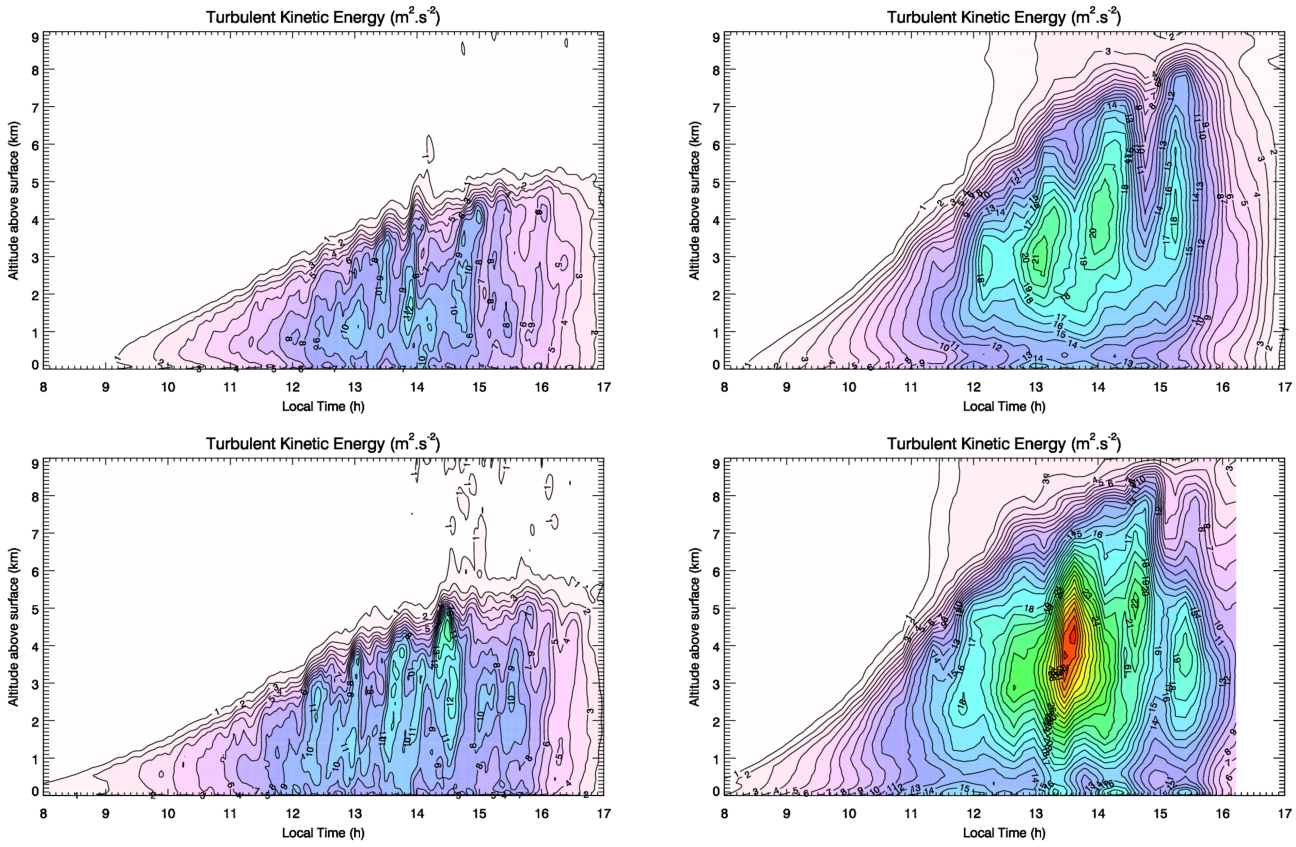

Figure 11. LMD (left) and SwRI (right) variations of turbulent kinetic energy between local times 07:00 and 19:00 and altitudes above ground 0 and 9 km. Simulations without ambient wind (top) and with 15 m.s^{-1} ambient wind (bottom).

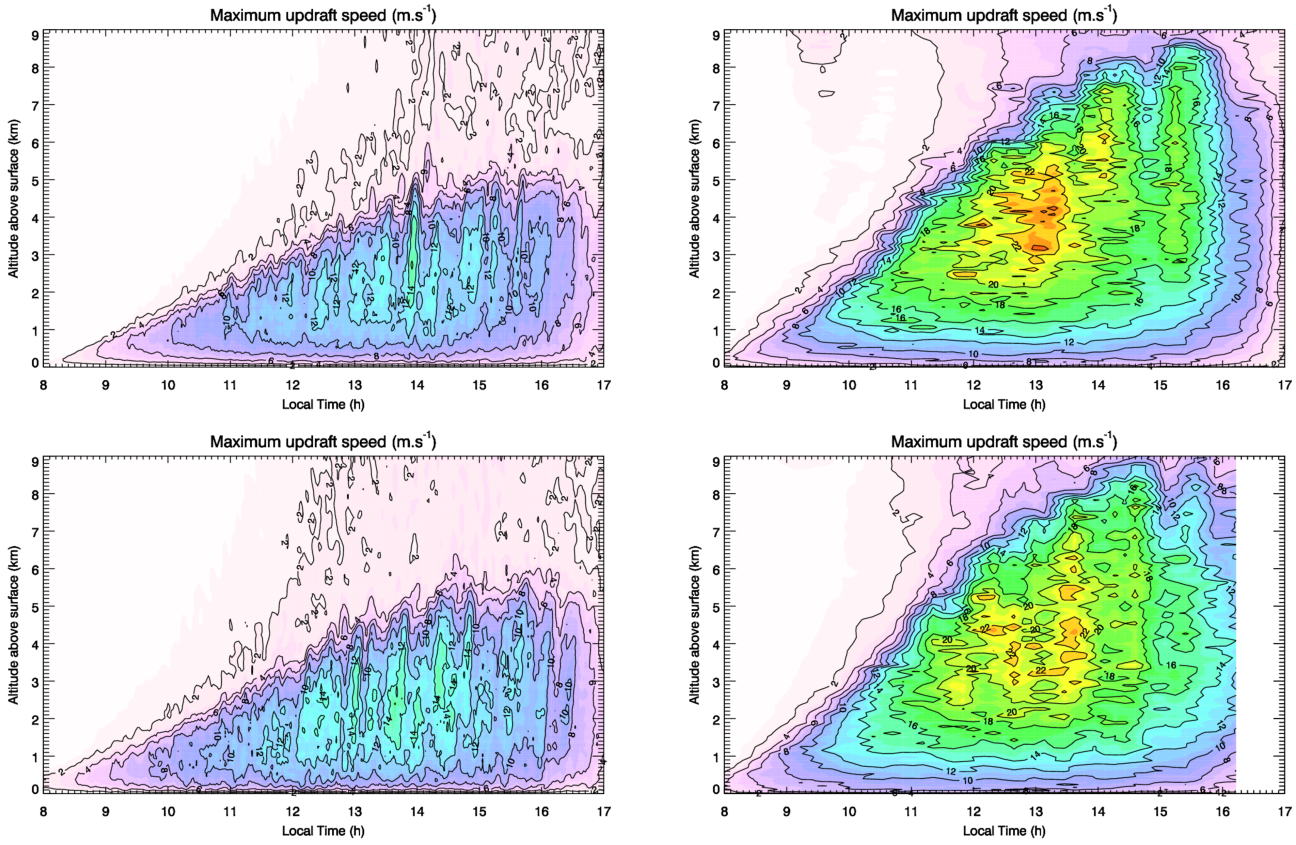

Figure 12. LMD (left) and SwRI (right) maximum speeds for convective updrafts reached in the simulation domain between local times 11:00 and 17:00 and altitudes above ground 0 and 8 km. Simulations without ambient wind (top) and with 15 m.s^{-1} ambient wind (bottom).

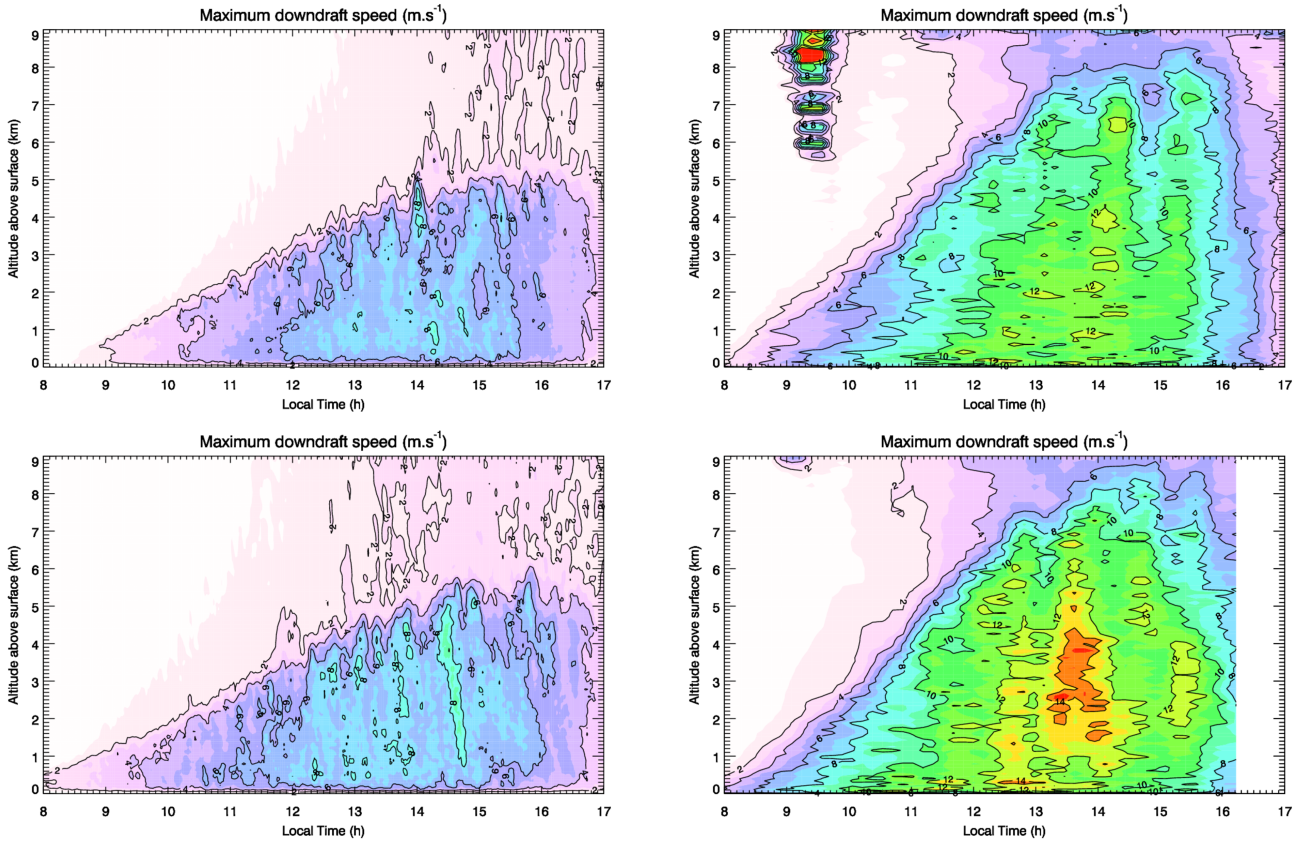

Figure 13. LMD (left) and SwRI (right) maximum speeds for convective downdrafts reached in the simulation domain between local times 11:00 and 17:00 and altitudes above ground 0 and 8 km. Simulations without ambient wind (top) and with 15 m.s^{-1} ambient wind (bottom).

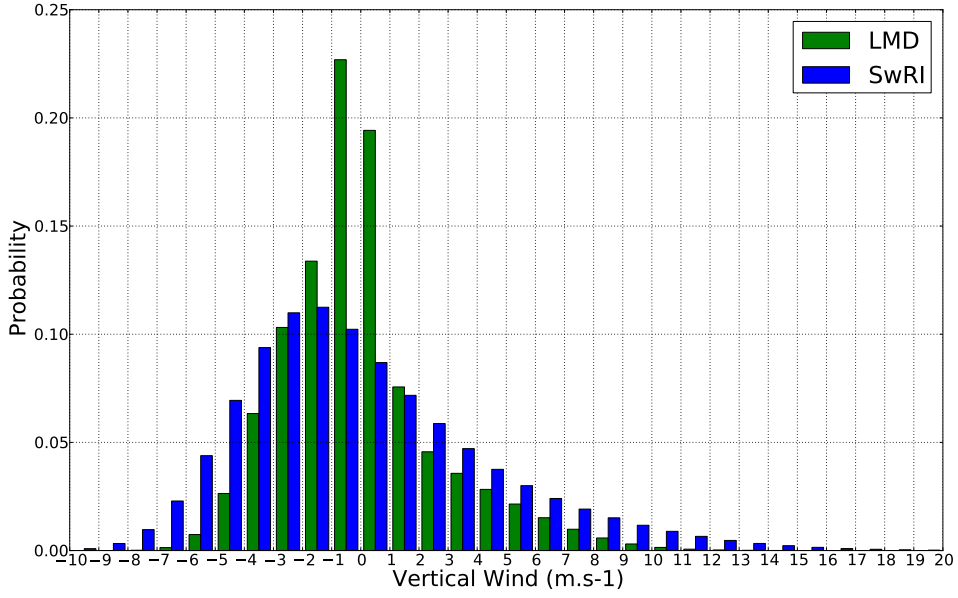

Figure 14. Histogram of vertical wind speeds for local times 13:00-14:00 and altitudes 250-5000 m. LMD results are in green, SwRI results are in blue. No ambient wind.

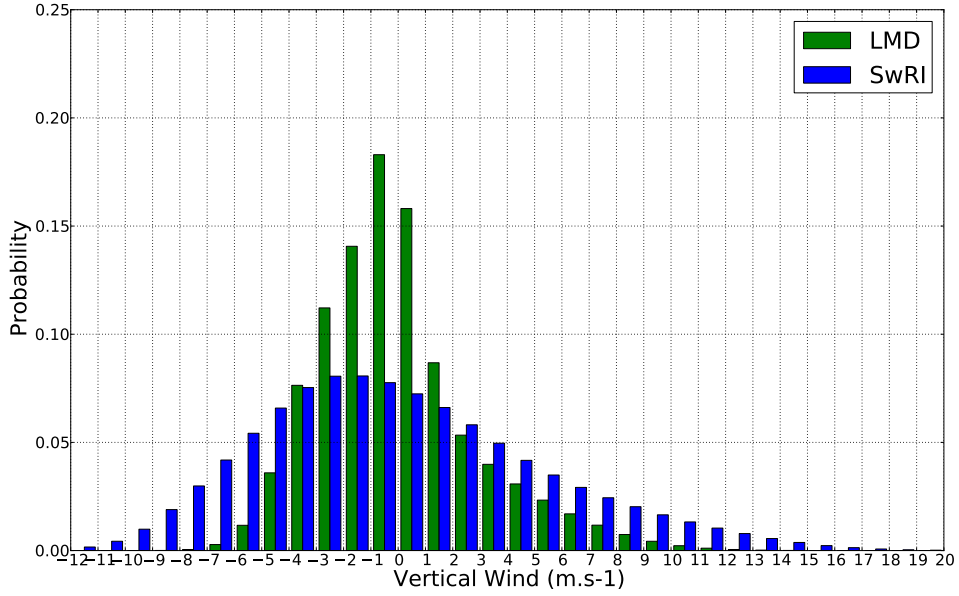

Figure 15. Histogram of vertical wind speeds for local times 13:00-14:00 and altitudes 250-5000 m. LMD results are in green, SwRI results are in blue. With 15 m.s^{-1} ambient wind.

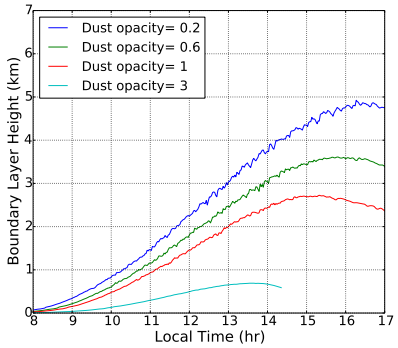

Figure 16. Evolution of the boundary layer depth for different dust optical depths (LMD LES)

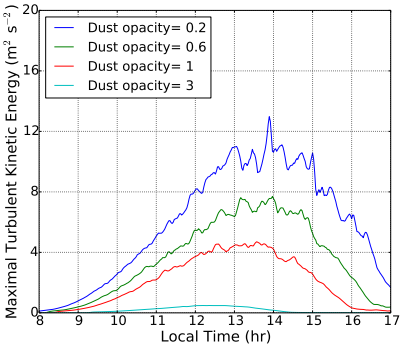

Figure 17. Evolution of the maximum turbulent kinetic energy for different dust optical depths (LMD LES)

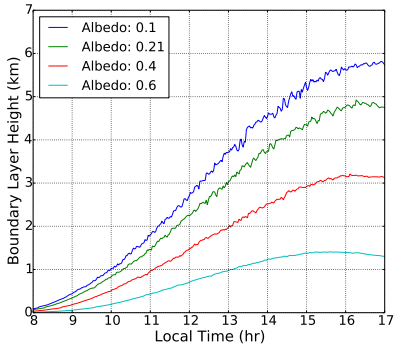

Figure 18. Evolution of the boundary layer depth for different surface albedo values (LMD LES)

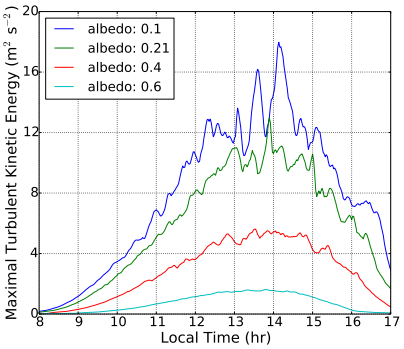

Figure 19. Evolution of the maximum turbulent kinetic energy for different surface albedo values (LMD LES)

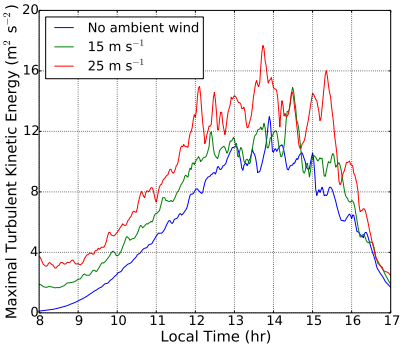

Figure 20. Evolution of the maximum turbulent kinetic energy for different large scale ambient winds (LMD LES)

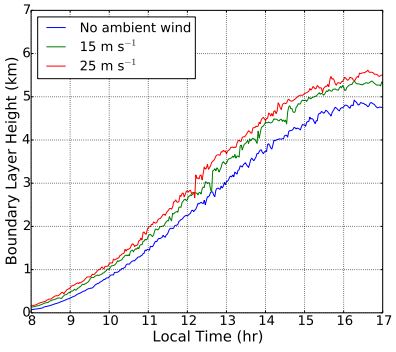

Figure 21. Evolution of the boundary layer depth for different large scale ambient winds (LMD LES)

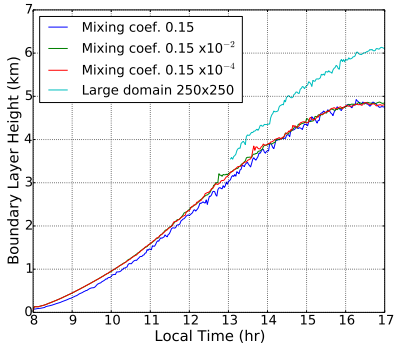

Figure 22. Evolution of the ~~maximum turbulent kinetic energy~~ boundary layer depth for different ~~large~~ subgrid scale ~~ambient winds~~ mixing coefficient and a case of larger domain (LMD LES). The fist part of the curve of the larger domain simulation is missing because of technical issues but this does not alter the comparison made in the afternoon.